AIChE

Kinetics of Adsorption of 2-CEES and HD on Impregnated Silica Nanoparticles Under Static Conditions

Amit Saxena, Avanish Kumar Srivastava, and Beer Singh
PD Div., Defence R & D Establishment, Jhansi Road, Gwalior 474002, MP, India

DOI 10.1002/aic.11741
Published online April 7, 2009 in Wiley InterScience (www.interscience.wiley.com).

Silica nanoparticles of high surface area (887.3 m^2/g) were synthesized using aerogel route and, thereafter, impregnated with those reactive chemicals, which have already been proven to be effective against sulfur mustard (HD). Thus, developed adsorbents were tested for their potential by conducting studies on kinetics of adsorption of 2-chloroethylethyl sulfide (2-CEES) and HD under static conditions. Kinetics of adsorption was studied using linear driving force model and Fickian diffusion model. The kinetic parameters such as equilibration constant, equilibration capacity, diffusional exponent, and adsorbate-adsorbent interaction constant were also determined. Trichloroisocyanuric acid impregnated silica nanoparticles (10% w/w) showed the maximum uptake of 2-CEES (1824 mg/g) and HD (1208 mg/g). Values of diffusional exponent indicated the mechanisms to be Fickian and anomalous. Chemical interaction seemed to be another mechanism involved in the toxicant uptake rate. Hydrolysis, dehydrochlorination, and oxidation reactions were found to be the route of degradation of toxicants. © 2009 American Institute of Chemical Engineers *AIChE J,* 55: 1236–1245, 2009
Keywords: metal oxide nanoparticles, impregnation, adsorption kinetics, degradation, toxic chemicals

Introduction

In recent years, the scientific community has shown increasing concern to find out the safe and effective ways to detoxify persistent chemical warfare (PCW) agents without endangering the human life or the environment. This situation needs the development of suitable real-time decontamination materials, which can perform in situ degradation (physisorption followed by chemisorption of the adsorbate) of PCW agents. Nanoparticles have received enormous interest recently because of their unique physical and chemical properties.[1] These materials have been synthesized via soft chemistry by sol-gel processes.[1] These metal oxides work as a destructive adsorbent due to its high surface area and chemical reactivity, i.e., initially the adsorbate molecules are physically adsorbed followed by dissociative chemisorption to such an extent that the chemical integrity of the adsorbate molecule is completely destroyed.[2,3]

Koper and Klabunde[4] have discussed the use of nanoparticles as destructive adsorbents for biological and chemical contamination. They have declared the preferred metal oxides as MgO, CaO, TiO_2, ZrO_2, FeO, V_2O_3, Mn_2O_3, Fe_2O_3, NiO, CuO, Al_2O_3, and ZnO, and their mixtures thereof; however, they have not used silica nanoparticles. As literature suggests[5] that single metal oxide particles show promising results, but these nanoadsorbents can further be modified for second generation nanoadsorbents by loading/impregnating with those reactive compounds,[6–9] which have already been proven to be active against CW agents, however, the possibility of new compounds for impregnation also exists. One such material, osmate stabilized on nanocrystalline magnesium oxide was prepared for achiral dihydroxylation of olefins to diols in the presence of a cooxidant.[5] Okun and Hill[8] have prepared the compositions of polyoxometalate/cationic silica material,

Correspondence concerning this article should be addressed to B. Singh beerbs5@rediffmail.com

copper salts, and combinations thereof to decontaminate 2-chloroethylethyl sulfide (2-CEES).

Impregnated nanoparticles based systems can be used to remove CW agents from solutions or contaminated air. The latter can be made breathable by allowing it to come in contact with nanoparticles based systems under dynamic (flow of gas) or static (no flow of gas) conditions. Under static conditions kinetics of adsorption and diffusion of adsorbate over adsorbent have widely been investigated.[6,7,10] Under these conditions the adsorption process involves the diffusion of adsorbate in micropores with pores widths considerably smaller than the mean free path of the gas molecules at atmospheric pressure. Therefore, if one bears in mind the pore size distribution in adsorbents, the modeling of the kinetic process becomes more difficult.[10]

Several researchers[6,7] have used various models, such as Fickian,[11] linear driving force (LDF),[12] a combined barrier resistance/Fickian diffusion, and Langmuir type second order kinetics[13] to describe the adsorption kinetics in porous materials and carbon molecular sieves. Chagger et al.[14] in 1995 discussed the kinetics of adsorption and diffusion characteristics on carbon molecular sieves using Ficks diffusion laws and linear driving force mass transfer model. Saxena et al.[7] studied the kinetics of adsorption of dimethylmethylphosphonate in gas phase on carbon systems under static conditions and determined various kinetics parameters such as equilibration time (t), equilibration capacity (M_t), rate constant (k), diffusional exponent (n), and constant (K).

When the adsorbate and adsorbent are at rest, i.e., under static conditions the distribution of adsorbate between gaseous and adsorbed phase is same throughout the layer of adsorbent. The behavior of vapor adsorption on nanoparticles based adsorbent system is decided by the nature of adsorbent surface, the time period for which the adsorbate molecule remains bound to adsorbent surface and the chemical reaction of adsorbate with impregnants on adsorbent surface. The time of adsorption depends upon the diffusivity of adsorbate molecules. Diffusivity is a function of surface concentration of adsorbate and the porous structure of the adsorbent.[15]

After adsorption kinetics the analysis of reaction/degradation products is equally important as that of kinetics study. Reactive adsorbents can degrade PCW agents by variety of reactions, such as oxidation, hydrolysis, elimination, addition, and dealkylation. In 2002, Narske et al.[16] performed the adsorptive removal of 2-CEES from solutions in pentane using AP-MgO. He indicated the formation of 2-HEES [(2-hydroxyethyl)ethyl sulfide] and ethylvinyl sulfide as reaction products. Room temperature destruction of HD [bis-(2-chloroethyl) sulfide] on nanoparticles of magnesium oxide[2] and aluminum oxide[3] has been widely investigated using solid state MAS-NMR techniques. Study indicated that hydrolysis of these agents took place on the surface of metal oxide nanocrystals and HD gets converted to thiodiglycol, 2-chloroethylvinyl sulfide, and divinyl sulfide.

As per above discussed literature either high surface area metal oxides/hydroxides (except silica nanoparticles) with reactive surfaces have been used alone or these have been mixed with decontamination solutions, foams, etc. for the degradation of PCW agents. *N*-chloro compounds[17] and *N*-sulphonyloxaziridines[18] have been widely used for the decontamination of PCW agents, but these have never been loaded on silica nanoparticles to degrade CW agents. This provides an open field for research and attracts attention for further work. If reactive nanoparticles have been impregnated with reactive chemicals then the chances of cross reaction do exist, this may destroy the activeness of both. Therefore, the use of inert high surface silica nanoparticles with reactive chemicals could be the most appropriate way to remove and detoxify PCW agents.

Inspired by this in the present study, AP-SiO_2 (aerogel produced silica) have been synthesized by aerogel-process[19] and subsequently characterized. Thereafter, to increase their reactivity these have been impregnated with trichloroisocyanuric acid, oxaziridine, sodium hydroxide, and ruthenium trichloride using incipient wetness technique. Later, these were explored to understand the adsorption kinetics of 2-CEES and HD, and to provide an insight to understand mass transfer phenomena, mode of diffusion, and adsorption characteristics.

Experimental

Synthesis of silicone oxide nanoparticles

AP-SiO_2 nanoparticles have been synthesized using ''bottom-up'' wet chemical method (aerogel process). For that 83.2 g of tetraethoxysilane was taken in a 1000 mL round-bottom flask having 500 mL of ethanol. To this 500 mL of toluene was added and the solution was stirred for 30 min under inert atmosphere of nitrogen gas. Thereafter, a solution of stoichiometric amount, i.e., 28.8 mL (1.6 M) of triple distilled and deionized water in 240 mL of ethanol and 735 mL of toluene was prepared. This solution was slowly added to the solution prepared in first step with vigorous stirring in 3.0 L round-bottom flask. The solution was covered with aluminum foil and stirred for 4 h. This resulted in opaque liquid-like gel.

Next 600 mL of thus formed silicon hydroxide gel was transferred to 1000 mL capacity parr autoclave. The gel was first flushed with inert gas and the reaction was carried out under inert gas with an initial pressure of 100 psi. The reactor was slowly heated from room temperature to 265°C at the rate of 1.0°C/min and the time of heating was 4 h. After reaching the desired temperature (265°C), the reactor was maintained at this temperature for 10 min. During heating the pressure inside the autoclave was increased to 800 psi. The system was quickly vented to the atmosphere for over a period of 1 min. The furnace was taken off and the produced powder was flushed with inert gas for 15 min to remove the remaining solvent vapors. The autoclave was allowed to cool to room temperature over ~3 h. After that thus produced material was thermally treated. For that, 25 g of thus produced powder was placed in 500 mL capacity thermal reactor. This was evacuated for 30 min at room temperature. Later, it was slowly heated for 6 h from room temperature to 500°C under dynamic vacuum of 10^{-2} Torr and kept under this condition for 10 h. Finally, the material was cooled to room temperature under vacuum, flushed with inert gas, and stored in airtight bottles till further use.

Loading of impregnants on silica nanoparticles

To prepare impregnated silica nanoparticles, AP-SiO_2 was impregnated (10% w/w) with trichloroisocyanuric acid, oxaziridine, $RuCl_3$, and NaOH separately. Impregnants in

Table 1. Surface Area, Pore Size Distributions, Bulk Density, and Moisture Content of Prepared Adsorbents

Prepared Adsorbent	Surface Area (N_2 BET) (m^2/g)	Micropore Volume (N_2 DR) (cm^3/g)	Cumulative Desorption Pore Volume (N_2 BJH) (cm^3/g)	Pore Maxima for Micro and Mesopores (Å)		Bulk Density (g/mL)	Moisture Content (%)
				Micro	Meso		
AP-SiO_2	887.3	0.386	1.451	14.6	27.5	0.035	0.8
AP-SiO_2 + TCCUA	682.9	0.302	0.839	15.1	24.5	0.048	1.9
AP-SiO_2 + $RuCl_3$	625.1	0.282	0.679	14.9	27.2	0.052	2.8
AP-SiO_2 + Oxaziridine	582.0	0.251	0.669	14.8	25.2	0.046	2.6
AP-SiO_2 + NaOH	120.6	0.049	0.166	15.1	27.5	0.102	1.9
CM-SiO_2	389.2	0.178	0.696	11.6	41.7	0.573	2.3

aqueous or organic solvent (corresponding to incipient volume of silica nanoparticles, i.e., 1 mL/100 mg silica) were used for the impregnation and the technique used for this was incipient wetness technique.[7] This technique allows the impregnant solution to just wet the adsorbent and allows the complete adsorption of impregnant on solid adsorbent. For impregnation the solution of trichloroisocyanuric acid in acetone; (1R)-(-)-(camphorylsulphonyl) oxaziridine in dichloromethane; $RuCl_3$ and NaOH in water were prepared. The impregnated systems were dried at 110°C for 4 h, cooled in desiccators, and finally stored in airtight bottles till further use.

Characterization of silica nanoparticles based adsorbents

Before use, silica nanoparticles with and without impregnants were characterized for porosity and surface characteristics using various techniques such as surface area analysis, scanning electron microscopy, transmission electron microscopy, powder X-ray diffraction, etc. The material was also characterized for acid/base neutralization capacity, bulk density, and moisture content.

Surface area and porosity

Surface area and pore size distribution of AP-SiO_2 (aerogel produced silica nanoparticles) and CM-SiO_2 (commercially available silica particles) were determined using Autosorb-1-C from Quantachrome, USA. The samples were first outgassed under dynamic vacuum (10^{-2} Torr) for 8 h at 200°C and then allowed to cool to room temperature. After that, the N_2 adsorption-desorption isotherms were obtained at liquid nitrogen temperature, i.e., 77 K. Surface area and micropore volume were determined using Brunauer-Emmet-Teller (BET) and Dubinin-Radushkevich (DR) methods, respectively. Cumulative desorption pore volume was determined using Barrett-Joyner-Halenda (BJH) method. Pore maxima for micro (<2 nm) and meso (2–50 nm) pores were determined considering BJH and DFT (density functional theory) methods. The surface area, micropore volume, cumulative desorption pore volume, and pore maxima for micropores and mesopores have been presented in Table 1. Figures 1 and 2 describe the nitrogen adsorption-desorption isotherms and pore size distributions of aerogel processed silica nanoparticles with and without impregnants.

Scanning electron microscopy/transmission electron microscopy and X-ray diffraction

For SEM characterization, the powder samples were first mounted on brass stubs using double sided adhesive tape and then gold coated for 8 min using ion sputter JEOL, JFC 1100 coating unit. The surface texture of silica nanoparticles was observed using FEI ESEM Quanta 400. Figure 3 represents the SEM image. TEM studies were performed to find out the particle size of the synthesized materials. For that 10 mg of sample was mixed in 10 mL of pentane and sonicated for 2 h to achieve a better separation of the particles. A drop of supernatant of the solution was placed on the

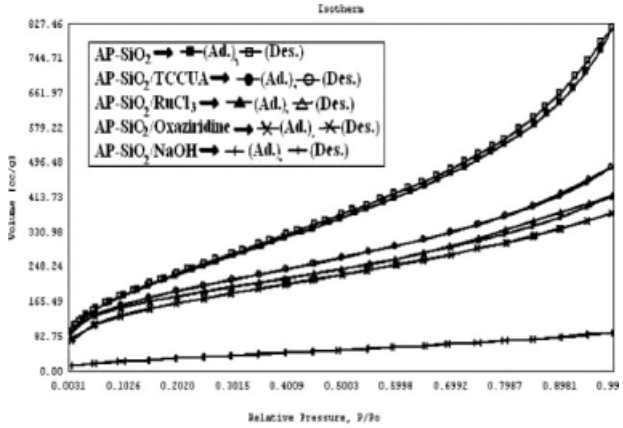

Figure 1. Adsorption isotherms of prepared adsorbents.

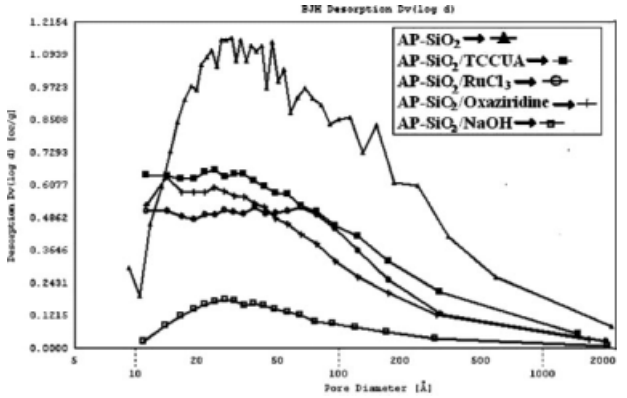

Figure 2. BJH pore size distributions of prepared adsorbents.

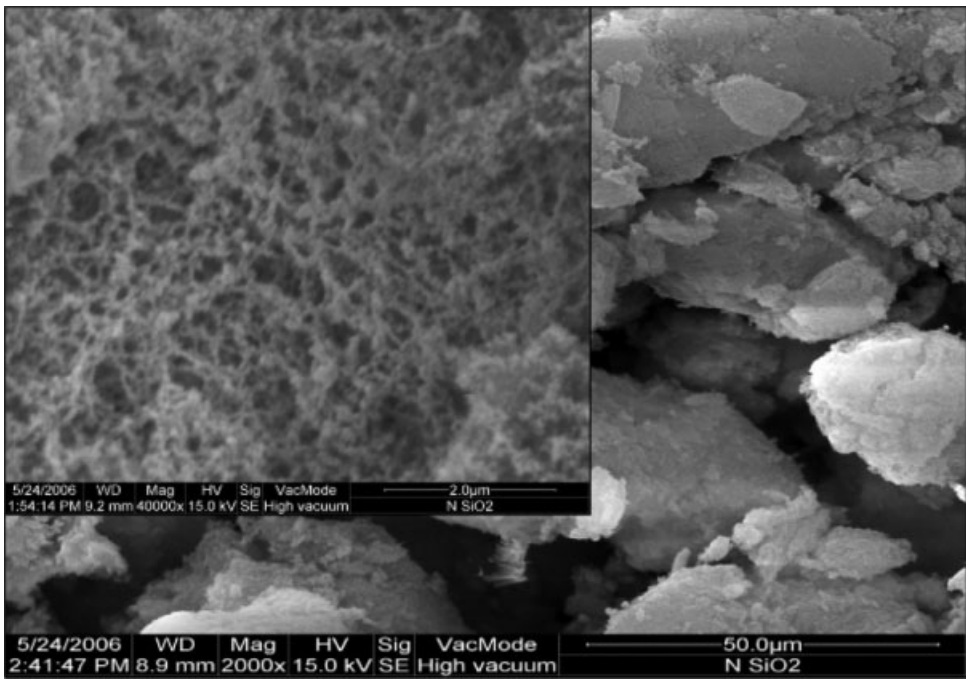

Figure 3. SEM image of silica nanoparticles.

copper grid of 200 mesh size followed by carbon coating. TEM images were recorded using JEOL, JEM-1200 Ex. Figures 4 and 5 represent the images. For XRD studies the powder samples were heat treated under vacuum before placing onto the sample holder. The instrument used was Philips XRD PW 3020. Cu Kα radiation ($\lambda = 0.154$ nm) was the light source used with applied voltage of 40 kV and current of 40 mA. The 2θ angles ranged from 20° to 80° with a speed of 0.05°/s. The crystallite size was then calculated from the XRD spectra using Scherrer equation.[20]

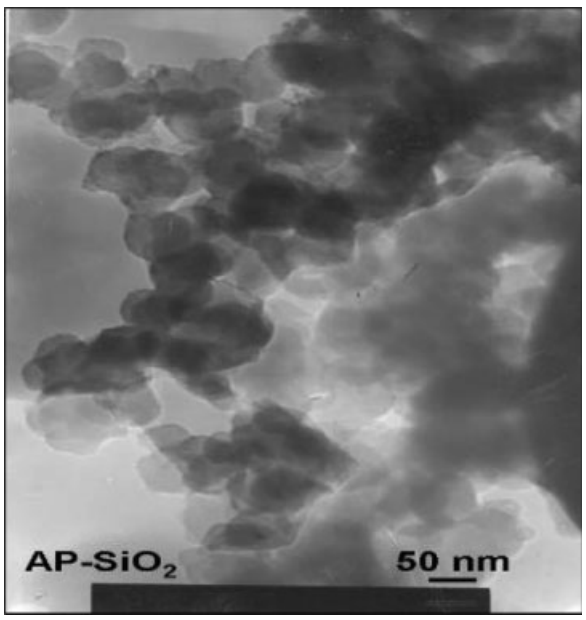

Figure 4. TEM image of silica nanoparticles.

Acid/base neutralization capacity, bulk density, and moisture content

To find out acid/base neutralization capacity of AP and CM-SiO_2, 20 mg of sample was taken in 20 mL of triple distilled and deionized water and stirred for 10 min. The pH of the solution was continuously noted. Then, it was titrated with 0.01 N HCl/NaOH till the pH of the solution reached to 6.5 (initial value of pH of distilled water). The bulk density of synthesized and commercial materials were measured by weighing a known volume (20 mL) of material and expressed in g/mL. The moisture content of the material was determined by heating a known amount (1 g) of sample in oven at 120°C for 6 h, cooling in desiccators for 1 h, and

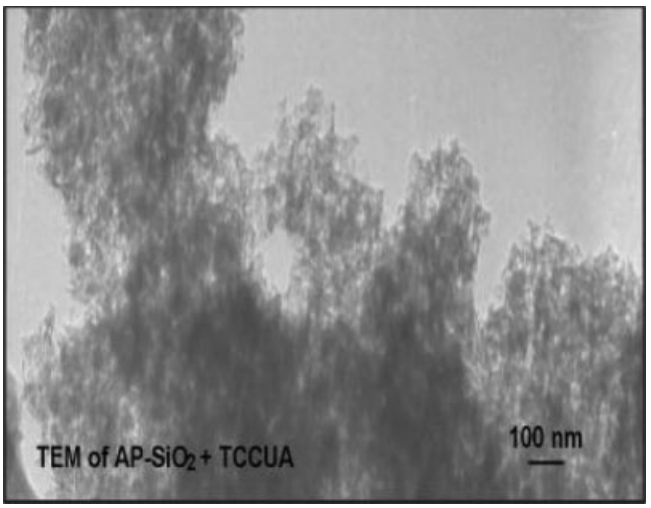

Figure 5. TEM image of trichloroisocyanuric acid impregnated silica nanoparticles.

finally weighing. The weight loss in sample per 100 g was taken as moisture content of the material. The bulk density and moisture content results have been described in Table 1.

Static adsorption studies

To carry out the adsorption of 2-CEES or HD under static conditions, 50 mg each of nanoparticles based adsorbent was taken separately in gooch crucibles and placed in desiccators in which 5.0 mL of 2-CEES or HD was placed in the bottom of desiccators. To maintain constant temperature, the desiccator was housed in an environmental chamber kept at 33°C ± 1°C. This chamber was used not only to control the temperature but also to house the weighing balance. Vapor pressure of 2-CEES and HD in the desiccators was measured and found to be 3.35 and 0.1 mm Hg at 33°C, respectively. The kinetics of adsorption of 2-CEES and HD was studied by monitoring the percentage of weight gain every hour. Figure 6 represents the kinetics of uptake of 2-CEES on prepared adsorbents. Figures 7 and 8 represent the kinetics of diffusion and adsorption of 2-CEES on prepared adsorbents respectively. Similarly, Figures 9–11 represent the kinetics of uptake, diffusion, and adsorption of HD on prepared adsorbents, respectively. Tables 2 and 3 represent the kinetics parameters.

Identification of reaction products

To investigate the reaction products, 10 mg of toxicant-exposed nanoparticle-based adsorbents were extracted with 2.0 mL of acetonitrile for 2 h in a well stoppered test tube. The extracts were centrifuged and transferred to another tube. The extracts were then purged with a slow flow nitrogen gas to concentrate the extracted reaction products and subjected to product identification using GC/MS (gas chromatograph coupled with mass spectrometer) instrumental techniques. GC/MS (6890N GC coupled with 5973 inert MS detector) of Agilent Technologies, USA was used for characterization of reaction products. It was equipped with HP-5 MS column of 30 m × 0.25 mm × 0.25 μ dimensions. Temperature programming [50 (2 min hold) to 280°C (10 min hold) at the rate of 10°C/min] with split injection technique (10:1) was used to perform the study. Injection port and GC/MS interface, MS source, and quadrupole analyzer were kept at 280, 230, and 150°C, respectively.

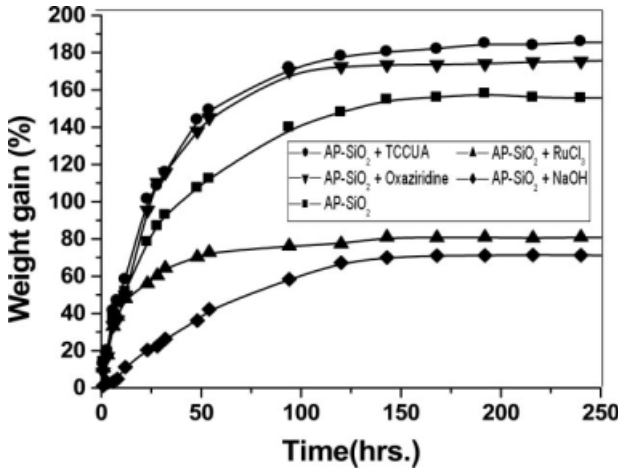

Figure 6. Kinetics of uptake of 2-CEES on prepared adsorbents.

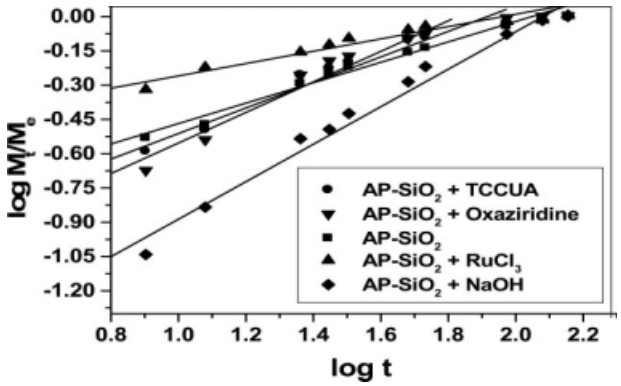

Figure 7. Kinetics of diffusion of 2-CEES on prepared adsorbents.

Results and Discussion

Characterization of silica nanoparticles based adsorbents

AP-SiO_2 showed highest uptake of nitrogen and exhibited hysteresis loop, which is the characteristic of adsorption possessing a portion of mesopores with mesopore maxima at 27.5 Å (Figure 1 and Table 1). Apart from mesoporous characteristics, AP-SiO_2 was also found to be having micropores with micropore maxima at 14.6 Å. The surface area of AP-SiO_2 was found to be 887.3 m^2/g, which was more than double of its counterpart, i.e., CM-SiO_2 (surface area = 389.2 m^2/g). This was in close association to that of BJH cumulative desorption pore volumes (AP-SiO_2 = 1.451 cc/g and CM-SiO_2 = 0.696 cc/g). Micropore and cumulative desorption pore volume of AP-SiO_2 were found to be 0.386 and 1.451 cc/g, respectively. When AP-SiO_2 was impregnated with trichloroisocyanuric acid (10% w/w), surface area decreased to 682.9 m^2/g (Table 1). This decrease was due to impregnants, which during impregnation travel through the macropores and gets deposited in the mesopores or the pore opening of micropores to cause the blocking of the meso/

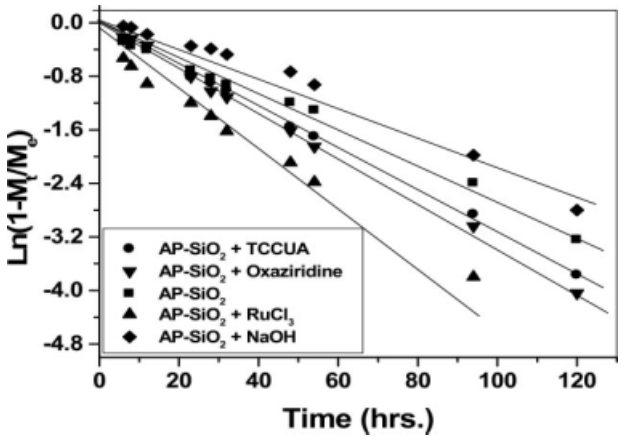

Figure 8. Kinetics of adsorption of 2-CEES on prepared adsorbents.

Table 2. Kinetics Parameters for the Adsorption of 2-CEES on Prepared Adsorbents

Prepared Adsorbent	Equilibration Time (h)	Equilibration Capacity (mg/g)	Rate Constant (k) (h^{-1}) ($\times 10^{-2}$)	Constant (K) (h^{-1})	Diffusional Exponent (n)	Surface Area (N_2BET) (m^2/g)
AP-SiO_2	144	1540	2.6	0.28	0.45	887.3
AP-SiO_2 + TCCUA	190	1824	3.2	0.24	0.58	682.9
AP-SiO_2 + Oxaziridine	121	1720	3.5	0.21	0.71	582.0
AP-SiO_2 + $RuCl_3$	140	801	5.0	0.49	0.27	625.1
AP-SiO_2 + NaOH	140	698	2.2	0.09	0.79	120.6

micropores.[7] Decrease in the surface area after impregnation was found with all samples (Table 1). Micropore (N_2-DR) and cumulative desorption pore volume (N_2-BJH) of AP-SiO_2 were also found to be decreased after impregnation (Table 1). AP-SiO_2 with NaOH impregnations (10% w/w) showed maximum reduction in surface area, i.e., from 887.3 to 120.6 m^2/g. This was probably due to the reaction of SiO_2 with NaOH to result sodium silicate. All impregnated silica samples showed strong mesoporous characteristics. Apart from mesoporous characteristic they were also found to be having micropores. Figure 2 clearly indicated that all nanosilica samples have the same type of pore size distributions with micropore and mesopore maxima at ~15 and ~25 Å (Table 1), respectively.

Figure 3 represents the SEM image of AP-SiO_2. The image clearly indicated the web/net like structure of nanoparticle aggregates with a quantum of huge porosity, which is confirmed by the surface area value of 887.3 m^2/g. TEM image of AP-SiO_2 (Figure 4) indicated the particle size of the particles to be 24 to75 nm with maximum particles in the range of 30 to 40 nm, whereas using XRD spectra and Scherrer equation it was calculated to be 2 to 27 nm with maximum particles of 2 nm diameter. Overall, smallest particles were of 2 nm diameter, which aggregate into ~30 nm particles, and these particles weakly agglomerate in to a mass with large pores, where the pores are actually the space between the particles (as opposed to holes and channels in the particles themselves). These particles when impregnated with TCCUA the particle size changed to 38 to 90 nm (Figure 5) with maximum particles in the range of 45 to 55 nm.

Subsequently, the bulk density of impregnated silica nanoparticles based adsorbents was determined and found to be in the range of 0.046 (AP-SiO_2 + oxaziridine) to 0.102 (AP-SiO_2 + NaOH) g/mL (Table 1). AP-SiO_2 indicated the increase in bulk densities after impregnation due to the reason that impregnants sit in the pores, the outer surface volume of the material remains same, whereas weight increases due to impregnation, and hence density increases. A threefold increase (from 0.035 to 0.102 g/mL) in bulk density of AP-SiO_2 + NaOH system has also indicated the reaction of SiO_2 with NaOH as that of indicated by decrease in surface area values. Moisture content (Table 1) of all prepared systems was found to be in the range of 0.8 to 2.8% (w/w).

Kinetics of adsorption of 2-CEES

To illustrate the kinetics of adsorption of 2-CEES, percentage weight gain of adsorbate was plotted vs. time (t) and represented graphically in Figure 6. Since moisture free air was not used to monitor the kinetics of adsorption of 2-CEES, the possibility of coadsorption of atmospheric moisture cannot be ruled out. However, the coadsorption of water will be insignificant and will not affect the adsorption of 2-CEES due to very little influence of humidity on adsorption of CW agent simulants.[21] Of the above; the concentration of gas was considered to be constant at atmospheric pressure in the desiccators. As the adsorption of toxicant by the nanoparticles based adsorbents starts it causes the depletion in vapor phase concentration of toxicant in the desiccators. The depletion in concentration is compensated by liquid phase toxicant, which was placed in the bottom of the desiccators. Therefore, the concentration of toxicant vapor in the desiccators remains constant and it ensures a continuous supply of toxicant to the adsorbent. Figure 6 shows the similar shape of 2-CEES adsorption uptake curves and different adsorption rates for studied nanosilica-based adsorbent systems. At initial stage the rate of adsorption was fast, which gradually slowed down to a steady state at later intervals of time. Except AP-SiO_2 + NaOH system the rate of adsorption of 2-CEES by the adsorbents was found to be same at initial stages (up to 10 h). Thereafter, the rate of adsorption varied and AP-SiO_2 + TCCUA system showed maximum uptake of 2-CEES amongst other systems.

Figure 6 was used to compute the equilibration time (the time at which the adsorption ceases, i.e., no change in weight gain with respect to time) and equilibration capacity (amount of adsorbate in mg/g of adsorbent at equilibration time), and the values have been tabulated in Table 2. AP-SiO_2 + TCCUA and AP-SiO_2 + oxaziridine system showed the highest and lowest values of equilibration time, respectively, whereas AP-SiO_2 + TCCUA and AP-SiO_2 + NaOH system showed the maximum and minimum equilibration capacity. The equilibration capacity always depends upon

Table 3. Kinetics Parameters for the Adsorption of HD on Prepared Adsorbents

Prepared Adsorbents	Equilibration Time (h)	Equilibration Capacity (mg/g)	Rate Constant (k) (h^{-1}) ($\times 10^{-2}$)	Constant (K) (h^{-1})	Diffusional Exponent (n)	Surface Area (N_2BET) (m^2/g)
AP-SiO_2	261	1043	1.75	0.18	0.56	887.3
AP-SiO_2 + TCCUA	412	1208	0.98	0.09	0.71	682.9
AP-SiO_2 + Oxaziridine	558	1112	0.85	0.08	0.77	582.0
AP-SiO_2 + $RuCl_3$	120	618	2.04	0.17	0.58	625.1
AP-SiO_2 + NaOH	315	202	1.49	0.28	0.36	120.6
CM-SiO_2	150	592	2.33	0.14	0.70	389.2

the surface area of the adsorbents, higher the surface area higher will be the adsorption capacity. This was found to be true with $RuCl_3$ and NaOH impregnated nanosilica-based systems, whereas TCCUA and oxaziridine impregnated systems showed higher adsorption capacities than their corresponding unimpregnated base material, i.e., nanosilica with even higher surface area values. AP-SiO_2 showed 23% decrease (887.3 to 682.9 m^2/g) in surface area after impregnation with TCCUA (AP-SiO_2 + TCCUA system), whereas adsorption capacity increased by 18% after impregnation (Table 2). It clearly indicated the important role of TCCUA in adsorption kinetics. This interesting behavior of high adsorption potential with lesser surface area indicates the adsorption by AP-SiO_2 + TCCUA system was not only due to physisorption but also involved chemisorption, where the physisorbed 2-CEES molecules diffused to the chemisorption sites and gets reacted with the impregnants, ultimately resulting in the increased adsorption potential. Saxena et al.[7] have also observed higher adsorption capacities with impregnated adsorbents for the adsorption of dimethylmethylphosphonate on impregnated carbons. Contradictorily to the above, AP-SiO_2 + $RuCl_3$ system showed adsorption capacity ~50% of that of AP-SiO_2 + TCCUA or AP-SiO_2 + oxaziridine systems, whereas the surface area was nearly similar for them (Table 2). The reason for less adsorption potential could not be understood. Overall, this indicated that rutheniumtrichloride impregnation to silica nanoparticles is not supportive for the adsorption of 2-CEES.

The study indicated that the transport of 2-CEES into nanoadsorbent systems is a complex process. It is quite evident from the fact that metal oxide nanoparticles contain wide pore size distribution, which makes the analysis of adsorption kinetics more complex. The adsorption process involves diffusion in slit-shaped micropores with pore widths considerably smaller than the mean free path of the gas molecules at atmospheric pressure.[14] It is likely that processes such as molecular diffusion, Knudsen diffusion, surface diffusion, diffusion in micropores, and the chemical interaction of 2-CEES with the functional groups of nanoparticles and the impregnants in it could all make contributions to the adsorption kinetics.

Modeling of kinetic process being difficult due to wide pore size distribution, the two simple approaches are to use either Ficks diffusion laws for homogeneous materials or to describe the process by Phenomenological model. Although, the particles under study are not homogeneous and spherical, if we assume surface concentration of gas to be constant and that diffusion is controlled by the concentration gradient through the granule then the kinetics of the diffusion can be expressed by the following empirical diffusion equation.[14,22]

$$M_t/M_e = Kt^n \tag{1}$$

where M_t = gas uptake at time t, M_e = gas uptake at equilibrium, K = constant, t = time, and n = diffusional exponent.

A graph of log M_t/M_e against log t (Figure 7) was found to be a straight line at shorter intervals of time and the plots deviated from linearity for all the systems at higher t values. This deviation can be ascribed to the wide pore size distribution of prepared systems (Figure 2). The diffusional exponent (n) values were computed by using the slope of straight line in Figure 7. For $RuCl_3$ impregnated and unimpregnated silica, n values were found to be 0.27 and 0.45, respectively (Table 2). Values of n being <0.5 indicated the diffusion mechanism to be Fickian.[11] TCCUA-, NaOH-, and oxaziridine-impregnated nanosilica particles indicated the values of n between 0.5 and 1.0, which indicated the diffusion mechanism to be anomalous.[11] The value for constant K, adsorbate-adsorbent interaction coefficient, was determined from the intercept of straight line on Y-axis. K represents the interaction between adsorbate and adsorbent, i.e., higher the K values higher will be the interaction of adsorbate with adsorbent. The K values determined from Figure 7 were more or less the result of adsorption kinetics at lower t values. In present study AP-SiO_2 + $RuCl_3$ and AP-SiO_2 + NaOH system showed the highest and lowest value of K (0.09 and 0.49 h^{-1}) respectively, whereas other systems showed small differences in K value and may be within the experimental precision. Highest value of K with $RuCl_3$-impregnated silica nanoparticles based system further emphasized the interaction of impregnant with adsorbate. This has also been supported by fastest initial adsorption kinetics (Figure 6, ~50 and ~95% adsorption within 10 and 40 h, respectively).

The gas uptake into nanoparticles may be considered as a pseudo-first-order mass transfer between the gas phase and the adsorption sites.[14,22] The following phenomenological model, which is equivalent to a linear driving force mass transfer model, can represent the rate of uptake of toxicant.

$$M_t/M_e = 1 - e^{kt} \tag{2}$$

where k is rate constant.

Plots of ln $(1 - M_t/M_e)$ against time t (Figure 8) result in a straight line, which clearly indicated that the adsorption of 2-CEES on silica nanoparticles with and without impregnants follows LDF mass transfer kinetic model. Pore size distribution being wide in the studied systems could not adversely affect the applicability of the LDF model at initial intervals of time; however, at longer intervals of time, the curves obtained by making use of the LDF model deviated from linearity, questioning its applicability. Nevertheless, the initial linear portions can be used to evaluate the adsorption parameters, which make the LDF model persuasive. Using LDF model, the adsorption kinetics can be compared in terms of the rate constant (k), which indicates the rate of adsorption of 2-CEES as the system approaches to equilibrium. Rate constant, k, can either be determined from the gradient of the kinetic plot as shown in Figure 8 or by fitting the adsorption uptake curves to Eq. 2. Maximum and minimum values for rate constant k (Table 2) were found to be in similar order as that of K values. Lower value of k with AP-SiO_2 + TCCUA system was because of Figure 8, which more or less represents the adsorption kinetics at lower t values. Higher equilibration time with this system also lowered the rate constant. AP-SiO_2 + NaOH system again showed the lower value of rate constant k indicating slowest kinetics. Based on these results it can be inferred that AP-SiO_2 + TCCUA system (with maximum adsorption potential and considerable values of k/K) is the best system for the removal of toxicants gases from simulated contaminated zones (as 2-CEES vapors in closed desiccators).

Kinetics of adsorption of HD

To understand the kinetics of adsorption of HD, a graph of percentage weight gain of adsorbate vs. time was plotted (Figure 9). AP-SiO_2 system showed fastest uptake of HD among all systems at initial intervals of time, whereas AP-SiO_2 + TCCUA system crossed it at 175 h and ended with maximum adsorption capacity (Table 3). AP-SiO_2 system showed better performance than that of CM-SiO_2, whereas AP-SiO_2 + NaOH system again showed least potential, which was also in agreement with its surface area value. AP-SiO_2 + TCCUA system showed higher value of equilibration time (412 h) than AP-SiO_2 without impregnation (261 h) indicating the role of impregnants, which possibly have worked as a barrier and slowed down the adsorption kinetics. AP-SiO_2 + $RuCl_3$ system showed same adsorption capacity, i.e., ~50% of that of AP-SiO_2 + TCCUA or AP-SiO_2 + oxaziridine systems as that with 2-CEES adsorption.

Figure 10 describes the kinetics of diffusion of HD on nanosilica-based systems. Diffusional exponent (Table 3) for AP-SiO_2 + NaOH was found to be 0.36 indicating the diffusion mechanism to be Fickian, whereas, other systems with n values being in the range of 0.56 to 0.77 indicated the diffusion mechanism to be anomalous.[11] The K and k values were determined using Figures 10 and 11. When three systems, i.e., AP-SiO_2, AP-SiO_2 + TCCUA, and AP-SiO_2 + oxaziridine were compared in terms of K and k values then highest values were obtained with AP-SiO_2 system, indicating the fastest initial adsorption kinetics (clearly observed in Figure 9). AP-SiO_2 + TCCUA system showed the kinetics in between, whereas AP-SiO_2 + oxaziridine system showed the slowest adsorption kinetics among these systems (Table 3 and Figure 9). Although the extent of chemical interaction is large for impregnated silica nanoparticles, even then there is not much significant change in K values, indicating the invalidity of K values to predict the chemical interaction of the adsorbate with the impregnants present on the surface of the silica nanoparticles. Overall, the study clearly indicated that AP-SiO_2 + TCCUA system is the best system for the removal of HD from contaminated air (toxicant in air).

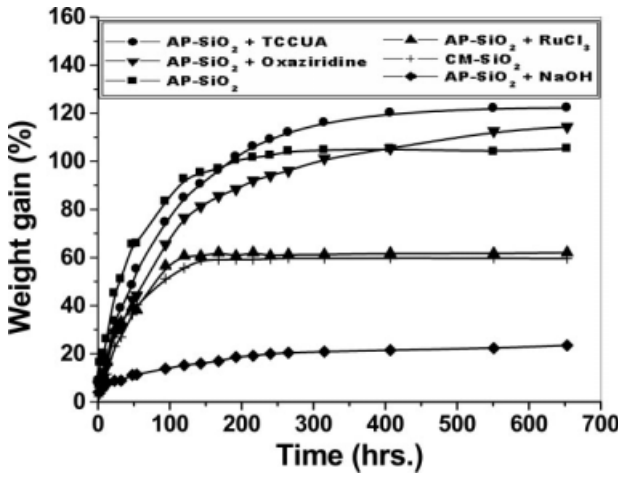

Figure 9. Kinetics of uptake of HD on prepared adsorbents.

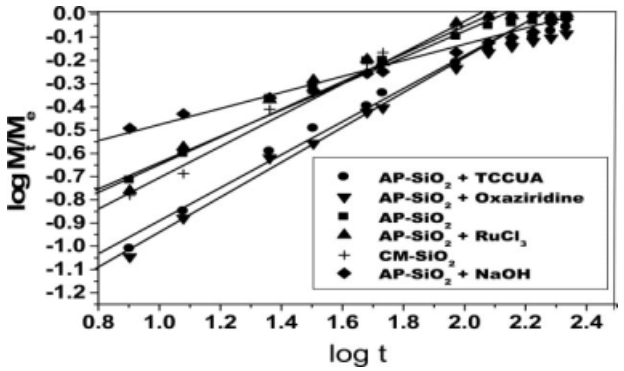

Figure 10. Kinetics of diffusion of HD on prepared adsorbents.

Identification of reaction products

The study on kinetics of adsorption of 2-CEES or HD indicated that the PCW agent molecules interact instantaneously with the active sites of the reactive metal oxide nanoparticles or impregnants and thereby made nontoxic due to the conversion of toxicants to nontoxic reaction products. To find out reaction products, these either have to be investigated directly using MAS-NMR technique[2,3] or by extracting them in organic solvent and analyzing through GC-MS.[23] As per literature[2,3] it is difficult to extract the reaction products from metal oxide nanoparticles because as the reaction product is generated, it bounds to the active site of metal oxide nanoparticles, thereby results to surface-bounded reaction products. In the present study reaction products have been identified using GC/MS analysis of extracts. The mass spectra of reaction products were compared with the standard mass spectra from existing libraries (Wiley and NIST) of GC/MS instrument.

All samples (AP-SiO_2, AP-SiO_2 + TCCUA, AP-SiO_2 + $RuCl_3$, AP-SiO_2 + oxaziridine, and AP-SiO_2 + NaOH) with and without impregnation (10% w/w) indicated the formation of 2-HEES (Scheme 1) as reaction product of 2-CEES. Results indicated that on the surface of AP-SiO_2 nanoparticles 2-CEES undergoes the hydrolysis reaction with the formation of intermediate sulfonium ion. Sulfonium ion is formed due to the attack of sulfide on the β carbon atom of 2-CEES and is considered to be SN^1 reaction. Sulfonium ion

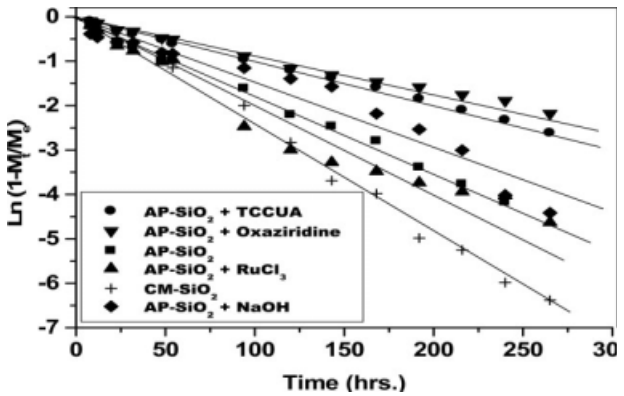

Figure 11. Kinetics of adsorption of HD on prepared adsorbents.

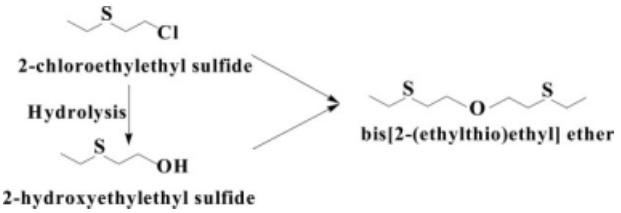

Scheme 1. Degradation products of 2-CEES on silica nanoparticles based adsorbent.

is highly unstable, because of which it could not be extracted and detected. Subsequently, the sulfonium ion undergoes hydrolysis with the water available with nanoparticles under study (no more water is added prior to the reaction) and gives rise to the formation of 2-HEES. Narske et al[16] has also indicated the formation of 2-HEES as reaction product of 2-CEES on nanocrystalline magnesium oxide. Moreover, the hydrolysis reaction of PCW agents on nanocrystalline metal oxides has been supported by Wagner et al.[2,3] Apart from that impregnated silica nanoparticles also indicated the formation of bis[2-(ethylthio)ethyl] ether as a reaction product, which is formed either via the combination of two 2-HEES molecules with removal of one water molecule or the combination of 2-CEES and 2-HEES (one molecule each) with the removal of HCl.

AP-SiO_2 indicated the formation of 2-chloroethylvinyl sulfide only as a reaction product of HD. When AP-SiO_2 was impregnated with trichloroisocyanuric acid (AP-SiO_2 + TCCUA), the system indicated hydrolysis (with the formation of intermediate sulfonium ion),[24] dehydrohalogenation, and oxidation reactions as a mode of degradation of HD (Scheme 2). Wagner et al.[2,3] have also indicated the hydrolysis and dehydrohalogenation reactions of HD on nanocrystalline metal oxides. Hemimustard (*m*/*z* values at 140, 109, 91, and 63, a hydrolysis reaction product of HD), chloroethylvinyl sulfide (via dehydrohalogenation reaction), and 1,4-oxathiane were observed as reaction products of HD. In addition to these products, oxaziridine and $RuCl_3$-impregnated silica nanoparticles indicated the formation of HD-sulfoxide (Scheme 2), an oxidation product of HD. The formation of oxidation product was due to the presence of impregnants ($RuCl_3$ and oxaziridine), which are already known for oxidation reactions.[18,25]

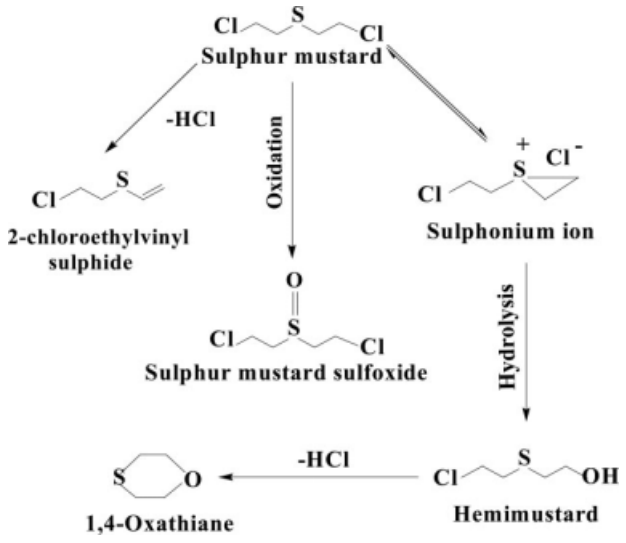

Scheme 2. Degradation products of HD on silica nanoparticles based adsorbent.

Conclusions

AP-SiO_2 nanoparticles with high surface area values and particle diameter in the range of 24–75 nm were synthesized using aerogel route. These were impregnated with reactive chemicals and subsequently characterized for porosity and surface morphology. Thereafter, studies on kinetics of adsorption of 2-CEES and HD on silica nanoparticles based adsorbents with and without impregnants were performed under static conditions to provide an insight to understand mass transfer phenomena, mode of diffusion, and adsorption characteristics. AP-SiO_2 + TCCUA and AP-SiO_2 + NaOH system showed the maximum and minimum equilibration capacity, respectively. Highest adsorption potential with AP-SiO_2 + TCCUA system indicated that the adsorption was not only due to physisorption but also involved chemisorption, where the physisorbed toxicant molecules diffuse to the chemisorption sites and react with the impregnants or active site of nanoparticle,[1–3] ultimately resulting in the increased adsorption potential. Although the extent of chemical interaction is large for impregnated silica nanoparticles, even then there is not much significant change in *K* values, indicating the invalidity of *K* values to predict the chemical interaction of the adsorbate with the impregnants present on the surface of the silica nanoparticles. TCCUA- and oxaziridine-impregnated nanosilica particles based systems showed the values of diffusional exponent (determined using Fickian diffusion model) in-between 0.5 and 1.0, indicated the diffusion mechanism to be anomalous.

All impregnated samples indicated the formation of 2-HEES and bis[2-(ethylthio)ethyl] ether as reaction product of 2-CEES. AP-SiO_2 + TCCUA system indicated the formation of 2-chloroethylvinyl sulfide, 1,4-oxathiane, and hemimustard as reaction products of HD. In association to this oxaziridine- and $RuCl_3$-impregnated silica nanoparticles indicated the formation of HD-sulfoxide. Moreover, AP-SiO_2 + TCCUA system showed highest adsorption potential against 2-CEES and HD, and degraded the toxicants to nontoxic reaction products. Overall, it can be inferred from the study that AP-SiO_2 + TCCUA system can promisingly be used in gas phase chemical warfare agent removal/decontamination devices and NBC filtration systems.

Acknowledgments

The authors thank Dr. R. Vijayaraghavan, Director, DRDE, Gwalior, for providing lab facilities to carry out and publish this work. They also thank Dr. M.V.S. Suryanarayana, Dr. K. Ganesan, and Dr. P. Pandey for useful suggestions.

Literature Cited

1. Klabunde KJ. *Nanoscale Materials in Chemistry*. New York: Wiley, 2001.
2. Wagner GW, Bartram PW, Koper O, Klabunde KJ. Reactions of VX, GD, and HD with nanosize MgO. *J Phys Chem B*. 1999;103: 3225–3228.

3. Wagner GW, Procell LR, O'Corner RJ, Munavalli S, Carnes CL, Kapoor PN, Klabunde KJ. Reactions of VX, GB, GD, and HD with nanosize Al_2O_3. Formation of aluminophosphonates. *J Am Chem Soc*. 2001;123:1636–1644.
4. Koper O, Klabunde KJ. Reactive nanoparticles as destructive adsorbents for biological and chemical contamination. US Patent WO 01/78506 A1, 2001.
5. Choudary BM, Jyothi K, Kantam ML, Sreedhar B. Achiral dihydroxylation of olefins by osmate (OsO_4^{2-}) stabilized on nanocrystalline magnesium oxide. *Adv Syn Catal*. 2004;346:45–48.
6. Prasad GK, Singh B, Saxena A. Kinetics of adsorption of sulfur mustard vapors on carbons under static conditions. *AIChE J*. 2006; 52:678–682.
7. Saxena A, Singh B, Sharma A, Dubey V, Semwal RP, Suryanarayana MVS, Rao VK, Sekhar K. Adsorption of dimethylmethylphosphonate on metal impregnated carbons under static conditions. *J Hazard Mater*. 2006;134:104–111.
8. Okun N, Hill CL. Materials for degrading contaminants. US Patent WO 03/094977A2, 2003.
9. Lomasney H, Lomasney C, Grawe J. Chemically and/or biologically reactive compounds. US Patent WO 03/092656A1, 2003.
10. Crank J. *The Mathematics of Diffusion*. Oxford: Clarendon Press, 1956.
11. Reid CR, Koye IPO, Thomas KM. Adsorption of gases on carbon molecular sieves used for air separation: spherical adsorptives as probes for kinetic selectivity. *Langmuir*. 1998;14:2415–2425.
12. Ulberg DE, Gubbins KE. Selective adsorption of vapors on graphitic carbon. *Mol Phys*. 1995;84:1139–1153.
13. Loughlin KF, Hassan MM, Fatehi AI, Zahur M. Rate and equilibrium sorption parameters for nitrogen and methane on carbon molecular sieve. *Gas Sep Purif*. 1993;7:264–273.
14. Chagger HK, Ndaji FE, Sykes ML, Thomas KM. Kinetics of adsorption and diffusional characteristics of carbon molecular sieves. *Carbon*. 1995;33:1405–1411.
15. Oscik J. *Adsorption*. Chichester: Illis Horwood, 1982.
16. Narske RM, Klabunde KJ, Fultz S. Solvent effects on the heterogenous adsorption and reactions of (2-chloroethyl)ethyl sulphide on nanocrystalline magnesium oxide. *Langmuir*. 2002;18:4819–4825.
17. Purdon JG, Chenier CL, Burczyk AFH. US Patent 6525237, 2003.
18. Davis FA, Haque SM. Oxygen transfer reaction of oxaziridines. In: Baumstark AL, editor. *Advances in Oxygenated Processes*. Greenwich, CT: JAL Press, 1990.
19. Koper OB, Lagadic I, Volodin A, Klabune KJ. Alkaline earth oxide nanoparticles obtained by aerogel methods. Characterization and rational for unexpectedly high surface chemical reactivities. *Chem Mater*. 1997;9:2468–2480.
20. Warren BE. *X-ray Diffraction*. New York: Dover, 1969.
21. Busmundrud O. Vapour breakthrough in activated carbon beds. *Carbon*. 1993;31:279–286.
22. Foley NJ, Thomas KM, Forshaw PL, Stanton D, Norman PR. Kinetics of water vapor adsorption on activated carbon. *Langmuir*. 1997;13:2083–2089.
23. Prasad GK, Mahato TH, Pandey P, Singh B, Suryanarayana MVS, Saxena A, Sekhar K. Reactivesorbent based on manganese oxide nanotubes and nanosheets for the decontamination of 2-chloroethylethyl sulphide. *Microporous Mesoporous Mater*. 2007;106:256–261.
24. Bartlett PD, Swain CG. Kinetics of hydrolysis and displacement reactions of b,b'-dichlorodiethyl sulfide (mustard gas) and of b-chloro-b-hydroxydiethyl sulfide (mustard chlorohydrin). *J Am Chem Soc*. 1949;71:1406–1415.
25. Sharma A, Saxena A, Singh B, Sharma M, Suryanarayana MVS, Semwal RP, Ganeshan K, Sekhar K. In-situ degradation of sulphur mustard and its simulants on the surface of impregnated carbon systems. *J Hazard Mater*. 2006;133:106–112.

Manuscript received Jan. 8, 2008, revision received Jun. 20, 2008, and final revision received Oct. 8, 2008.